

Suppressing AIM2/IL1 α /Piezo1 axis mitigates LPS-induced COPD in rats via targeting AMPK-dependent role of 5-aminolevulinic acid

Maram Mohammed El Tabaa^{a,*}; Manar Mohammed El Tabaa^b; Ahmed Almeldin^a; Hoda Ali Mohamed Ibrahim^c; Maram mofreh Mahrous Ghabrial^d, and Yasmeen M. El-Harty^a

^aMedical Physiology, Faculty of Medicine, Tanta University, Egypt;

^bPharmacology & Environmental Toxicology, Environmental Studies & Research Institute (ESRI), University of Sadat City, Sadat City 32897, Menoufia, Egypt.

^cAssistant professor of medical biochemistry and molecular biology, Faculty of Medicine, Tanta University, Egypt;

^dLecturer of anatomy and embryology, Faculty of Medicine, Tanta University, Egypt;

Submit Date : 30 Sept. 2024

Revised Date : 08 Dec. 2024

Accept Date : 10 Dec. 2024

Keywords

- 5-aminolevulinic acid
- Lipopolysaccharide
- Lung inflammation
- COPD
- AIM2/IL1 α /Piezo1 signaling axis

Abstract

Chronic obstructive pulmonary disease (COPD) is a serious respiratory disease with a rising incidence pattern. 5-aminolevulinic acid (5-ALA) has a potent anti-inflammatory effect, however, its impact on COPD has not been studied. Our aim is to investigate the involvement of AIM2/IL1 α /Piezo1 signaling axis in the pathogenesis of COPD produced by LPS in rats, as well as the potential alleviating effect of 5-ALA, via AMPK activation, against this pathway. Forty male rats were specified into four groups: normal control; 5-ALA; LPS; LPS+5-ALA. Gene expressions of AMPK, Nrf2 and Piezo1 were examined using RT-PCR quantification. Furthermore, lung protein expression of AIM2 inflammasome was assessed by western blotting. HO-1 levels, in addition to other oxidative stress and inflammatory markers were also detected. Histopathological examination and immunostaining of inflammatory markers (NF- κ B) were lastly determined. Our findings demonstrated that 5-ALA significantly upregulates AMPK, which in turn activating Nrf2/ Ho-1 axis with increased TAC levels and decreased ROS production. Through, 5-ALA prevented ROS overproduction, and subsequent AIM2/IL1 α /Piezo1 signaling. Consequently, NF- κ B activation and associated release of TNF- α and IL-6 were ultimately suppressed by 5-ALA. These results indicate that 5-ALA may possess a mitigating impact against inflammatory insult in COPD caused by LPS, via an AMPK-dependent mechanism, which is achieved by prohibiting AIM2/IL1 α /Piezo1 pathway.

Introduction

Chronic obstructive pulmonary disease (COPD) is a chronic inflammatory disease that affects peripheral airways and lung parenchyma, manifested as chronic obstructive bronchitis and emphysema[1]. By 2030, COPD is estimated to be ranked as the fourth most common cause of mortality globally[2]. It develops due to prolonged exposure to tobacco smoke, air pollution, occupational dust, harmful gases, fumes, etc[3]. Current pharmacological treatment for COPD includes the use of inhaled or oral corticosteroids and bronchodilators. Nevertheless, numerous categories of these drugs exhibit significant detrimental effects [1], so it is imperative to seek alternative therapy that decelerate COPD progression based on its fundamental cellular and molecular mechanisms.

Network analysis is a technique in system biology that uses computational techniques to look into novel treatment targets, processes, and unique protein-protein interactions[4]. In the lung, Piezo1 protein has been recognized to be highly expressed in alveolar epithelial cells, macrophages, and smooth muscle cells of small arteries, and it also plays a role in the process of vascular remodeling [5]. Piezo1 acts as an emerging regulator in macrophages, and associated inflammatory responses [6]. In addition, Piezo1 has been detected to activate nuclear factor kappa-B (NF- κ B) [7], which has a key role in the development of airways inflammation in COPD. It is activated in many types of cells in the airway, and thereby controls the expression of various inflammatory and immunomodulatory mediators [8]. Consequently, blocking the activation of Piezo1 could be applied as a potential strategy to reduce

inflammation and impede the progression of COPD. Nevertheless, its precise function remains unexplored.

Surprisingly, the expression and function of Piezo1 gene in chondrocytes has been reported to be mediated by IL-1 α [9]. At the same time, prior studies demonstrate the role of IL-1 α as a key mediator in the development of COPD[10, 11]. IL-1 α is mainly secreted by epithelial cells as well as macrophages, and its release is provoked by activating the absent in melanoma 2 (AIM2) inflammasome. During lung inflammation, AIM2 inflammasome has been found to be activated by macrophages. This activation leads to the generation of inflammatory mediators, stimulates the polarization of M1 macrophages, and eventually causes cellular inflammatory damage[12]. In addition, oxidative stress with reduced levels of antioxidants, as Nrf2, have a strong connection to inflammation in COPD[13]. Increased ROS production plays a vital role in the activation of AIM2 inflammasome[14].

Conversely, AMP-activated kinase (AMPK) has been documented to serve as a fundamental component for maintaining cellular energy balance. When AMPK is active, it produces several effects such as improved endothelial function, reduced inflammation, enhanced redox equilibrium, and promoted Nrf2 signaling[15]. The interplay between active AMPK and Nrf2 pathways has a significant impact on energy balance and antioxidative defense. This interaction may play a role in the development of innovative therapeutics for inflammatory illnesses[16]. Even so, the influence of AMPK on the AIM2/IL1 α /Piezo1 axis remains uncertain in the context of COPD pathogenesis.

Earlier, 5-Aminolevulinic acid (5-ALA) has been reported to be one of the compounds that activates AMPK signaling pathway [17]. 5-ALA is an endogenous amino acid that is synthesized within our body and can also be found in various food sources. It possesses anti-oxidant and anti-inflammatory properties [18, 19]. It has been documented that 5-ALA administration suppressed production of inflammatory cytokines and increased haem oxygenase-1 (HO-1), enhancing cellular antioxidant capacity [20]. However, in vivo effects of 5-ALA on COPD have not been investigated yet. Hence, it may be beneficial to elucidate the potential pharmacological mechanisms of 5-ALA against LPS-induced COPD, considering the possible AMPK role in suppressing AIM2/IL1 α /Piezo1 axis during the pathogenesis of this illness.

2. Materials and methods

2.1. Chemicals and reagents

Lipopolysaccharides from *Escherichia coli* (LPS; 297-473-0) and 5-aminolevulinic acid (5-ALA; 5451-09-2) were provided by Sigma-Aldrich Co. Inc., LouisSt., MO, USA. The spectrophotometric assay kits for malondialdehyde (MDA; MD 2529) and total antioxidant capacity (TAC; TA 2513) were provided by Bio-Diagnostics Co., Dokki, Giza, Egypt. The rat ELISA kits for peroxisome proliferator activated receptor gamma coactivator 1- α (PGC1- α , SEH337Ra), heme oxygenase-1 (HO-1, SEA584Ra), tumor necrosis factor- α (TNF- α , SEA133Ra), interleukin-6 (IL-6, SEA584Ra), and interleukin-1 α (IL-1 α , SEA071Ra) from Cloud-Clone Corp Co., Houston, USA. Moreover, rabbit polyclonal antibodies for activating the absent in

melanoma 2 (AIM2; #53491) was from Cell Signaling Technology, Inc., Massachusetts, USA.

2.2. Animals

The study was carried out on 40 male adult rats of local strain weighing (160-180 gm). Rats were housed in standard well-ventilated animal cages at room temperature, with free access to water and food throughout the entire period of work. The maximum number of rats per cage was assigned to three to avoid cage overcrowding or decreased cleanliness. Rats were monitored five times a week for signs of cage aggression or disease. All procedures were done according to the ethical committee of Tanta University (Approval Code Number: 36264PR841/9/24)

2.3. Experimental protocol

After one week acclimatization, the rats were randomly assigned to the following four groups ($n = 10$); **I-Normal control (C) group**: received once (50 μ L normal saline) per rat; intranasally (i.n.) and distilled water daily; orally for 14 days, **II-5-aminolevulinic acid (5-ALA) group**: received 30 mg/kg dissolved in distilled water daily (at concentration of 50 mg/ml); orally for 14 days [21], **III-Lipopolysaccharide (LPS) group**: received once (20 μ g lipopolysaccharide (LPS) dissolved in 50 μ L normal saline) per rat; intranasally (i.n.) [22], and **IV-LPS + 5-ALA group**: received LPS once and 5-ALA (at concentration of 50 mg/ml); orally for 14 days.

After twenty-four hours, 4 ml of ketamine/xylazine anesthetic solution/kg was i.p. injected into each rat. A sterile scissor was used to open the rat's chest and then, lungs of rats from each group was completely isolated. The bronchoalveolar lavage fluid (BALF) was collected from the left lungs, while the right

lungs were carefully dissected out and kept apart. Following dissection, lung tissue samples were divided into two portions. One portion was stored until used for polymerase chain reaction (PCR) technique and biochemical assays, but the other portion was used for histopathologic analysis.

2.4. Bronchoalveolar lavage fluid samples collection

After ligating the right main bronchus with 1-0 silk suture, all of the right lungs were removed and isolated. Then, all left lungs were lavaged three to five times with 30 mL of sterile saline/kg [23]. The bronchoalveolar lavage fluid (BALF) were thereby collected, centrifuged at $12,000 \times g$ for 30 min, and the supernatant were kept frozen at -20°C until used.

2.5. Network analysis

2.5.1. Defining the molecular targets connected to 5-aminolevulinic acid

The chemical structure of 5-ALA was retrieved in Canonical SMILES format from the PubChem database (**Supplementary Table S1**), (<https://pubchem.ncbi.nlm.nih.gov/compound/137#section=InChI>, accessed on 25 July 2024). Four datasets were then analyzed to determine the targets for 5ALA (**Supplementary Table S2**), as follows: (1) SwissTarget Prediction database (http://www.swisstargetprediction.ch/result.php?job=921332644&organism=Homo_sapiens, accessed on 25 July 2024); (2) SuperPred database (https://prediction.charite.de/subpages/target_result.php, accessed on 25 July 2024); (3) DrugBank (<https://www.syngoportal.org/convert>, accessed on 25 July 2024); and (4) The targetnet database (http://targetnet.scbdd.com/calcnnet/calc_text/,

accessed on 25 July 2024). Using the UniProt database (<https://www.uniprot.org/>, accessed on 25 July 2024), the targets retrieved from the four databases were standardized into legitimate gene symbols for additional research. All duplicate targets were eliminated by utilizing the Jvenn tool (<https://jvenn.toulouse.inrae.fr/app/example.html>, accessed on 25 July 2024).

2.5.2. Detection of targets linked to COPD

Four databases containing the molecular targets associated with the target diseases were searched using the phrase "chronic obstructive pulmonary disease or COPD" (**Supplementary Table S4**): (1) GeneCards database (<https://www.genecards.org/Search/Keyword?queryString=%22chronic%20obstructive%20pulmonary%20disease%22>, accessed on 25 July 2024); (2) The Open Targets Platform database, (https://platform.opentargets.org/disease/EFO_0000341/associations, accessed on 25 July 2024); (3) Comparative Toxicogenomics Database (CTD), (<https://ctdbase.org/detail.go?type=disease&acc=MESH%3AD029424&view=gene>, accessed on 25 July 2024); and (4) MalaCards database (https://www.malacards.org/card/pulmonary_disease_chronic_obstructive?search=chronic,obstructive,pulmonary,disease#Genes, accessed on 25 July 2024) [24]. The four databases offer additional resources to obtain targets relevant to diseases. Using UniProt, all targets were transformed into the universal gene symbol format, and any duplicate targets were removed.

2.5.3. Creation of disease-drug common targets, protein–protein interaction, and drug-target networks

The online Jvenn program was used to populate the empirically determined targets for

COPD and 5-ALA and produce a Venn diagram depicting their shared targets. The appropriate targets were uploaded to the STRING database Version 12.0 (<https://string-db.org/>, accessed on 26 July 2024) [25], in order to construct the protein–protein interactions (PPI) network of the intersected targets with a default confidence level of >0.4. Homo sapiens was a selected organism for analysis. A compound-target network was established to connect 5-ALA with numerous overlapping targets following the construction of the PPI network. The Cytoscape 3.10.2 program, created by NIGMS in the US, was used to visualize the network [26]. Next, the common overlapping targets were filtered by degree value and subsequently rated according to Betweenness and Closeness through using the Cytoscape plugin CytoNCA [27]. The hub targets were determined to be the top 10 ranking proteins.

2.5.4 Inspection of functional enrichment

The Gene Ontology (GO) analysis and Kyoto Encyclopedia of Genes and Genomes (KEGG) pathway enrichments were performed via applying the ShinyGO program (<http://bioinformatics.sdstate.edu/go/#tab-6415-3>, accessed on 26 July 2024)[28]. The cutoff value was set at a critical P value of less than 0.05. The outcomes were displayed by the ShinyGO website as lollipop charts for Gene Ontology (GO) terms and as Sankey and dot plots for KEGG pathways, as given by the SRplot website (<https://www.bioinformatics.com.cn/en?keywords=ENRICHMENT>, accessed on 26 July 2024)[29].

2.5.5. Molecular docking

As stated by[30], the following exact steps were taken to complete the molecular docking process: The 3D chemical structural model of 5-

ALA was downloaded in SDF format from the PubChem database (<https://pubchem.ncbi.nlm.nih.gov/>) and it was then converted to a PDB format using the Open Babel GUI application (version 2.4.1).

Additionally, the proteins PRKAA1, AIM2, and Piezo1 were chosen, and the Research Collaboratory for Structural Bioinformatics (RCSB)-Protein Data Bank (PDB) Database (<https://www.rcsb.org/>) was used to obtain the PDB format of their structures. The PyMOL 3.0 software was used to introduce polar hydrogen atoms into each target after eliminating their residue and water. To do computational docking, the EMPA molecule and targets files were loaded separately into PyRx (version 0.8). The combination modes and binding energy values with the best quality were then recorded. The unit of measurement for binding affinity is kcal/mol. Notably, a strong binding activity is indicated by values less than -7. Using the BIOVIA Discovery Studio 2024 Client software, the final visualization and analysis of the 2D force and 3D spatial environment images were carried out.

2.6. Analysis of lung oxidant/antioxidant status

MDA concentration (in nmol/mL) and TAC concentration (in mol/mL) were measured colorimetrically inBALF supernatant, using spectrophotometric assay kits at 534 nm and 505 nm, respectively [31, 32]. ELISATEchnology was used to measure the the lung concentration of HO-1 (in ng/mg tissue).

2.7. Analysis of lung inflammatory markers

The BALF concentrations of IL-1 α , IL6,and TNF- α in pg/mL will be measured according to the manufacturer's ELISA kit instructions.

Table 1: Real-time PCR (qPCR) primer pairs.

Gene	(NCBI GenBank nucleotide accession)	Primers	Amplicon size
Piezo 1 (ID: 9780)	NM_001142864.4	Forward: 5'-GGACTCTCGCTGGTCTACCT -3' Reverse: 5'-GGGCACAATATGCAGGCAGA -3'	171
Nrf2 (ID: 4779)	NM_003204.3	Forward: 5'-GACATGGATTTGATTGACAT -3' Reverse: 5'-CCTTCTCCTGTTCCCTTCTGG -3'	100
AMPK α (ID: 5562)	NM_006251.6	Forward: 5'-GGCAAAGTGAAGATTGGAGAACA-3' Reverse: 5'-AACTGCCACTTTATGGCCTGTC-3'	51
GAPDH (ID: 2597)	NM_002046.7	Forward: 5'- TGCCACTCAGAAGACTGTGG -3' Reverse: 5'- TTCAGCTCTGGGATGACCTT -3	129

2.8. Western blot analysis

After homogenising the frozen lung tissues using radioimmunoprecipitation assay (RIPA) buffer, the homogenates were centrifuged at 12000g for 15 min at 4 °C. Total protein was extracted from tissues using a protein extraction Kit (NBP2-37853) according to the manufacturer's guidelines (Novus Biologicals, LLC, USA). A PierceTM bicinchoninic acid (BCA) protein assay kit (Thermo Fisher Scientific Inc., USA) was used to determine the protein contents in tissue homogenates. The samples with the same concentration of 30 μ g per lane were added onto an SDS-PAGE 4-12% gel. After that, the proteins were transferred onto PVDF membranes. To determine the molecular weights of the proteins, we utilized prestained protein ladders (ab116028, Abcam, USA) with a wide range of molecular weights. A blocking solution (TBST) comprising 5% skim milk in Tris-buffered saline containing 0.05% (v/v) Tween 20 was used to obstruct the membranes at 25 °C for a period of 2 hours. Following this, the membranes were incubated overnight at a temperature of 4°C with the target

primary antibodies at a dilution of 1:1000, including (anti-AIM2 and anti-GAPDH).

The blotting membranes underwent three washes with TBST at 15-minute intervals on the subsequent day. Consequently, the samples were subjected to incubation with a secondary antibody, namely goat anti-rabbit IgG HRP-linked secondary (1:1000), at a temperature of 37 °C for a period of 1 hour. Finally, the bands were obtained and their density was quantified utilizing densitometry *ImageJ* software (the National Institute of Health in Bethesda, USA) and the relative protein expression was evaluated.

2.9. Assessment of AMPK, Nrf2, and Piezo1 gene expression using real-time RT-PCR

After the frozen lung tissue was processed following the manufacturer's instructions, total RNA was extracted using a Qiagen RNeasy Total RNA isolation kit (Qiagen, Hilden, Germany). Using a NanoDrop spectrophotometer (NanoDrop Technologies, Inc. Wilmington, USA), the total RNA concentration, purity, and integrity were determined. The RNA was subsequently kept at -80 °C using the OD260 and OD260/280 ratios, respectively. Power SYBR Green PCR Master Mix (Life Technologies, Carlsbad, California, USA)

was used to conduct the PCR experiments. As an internal control for a real-time PCR process, the housekeeping gene GAPDH's mRNA transcript levels were evaluated for Piezo1, Nrf2, and AMPK α (Table 2). Using the 2- $\Delta\Delta$ CT method and

the comparative threshold (Ct) approach, the relative gene expression was automatically calculated based on the values of the target and reference genes.

Table 2: Details of molecular docking between 5-aminolevulinic acid molecule and important targets

Molecule name	Targets	Gene name	PDB number	Binding ability (kcal/mol)
5-aminolevulinic acid (5-ALA)	AMP-activated protein kinase (AMPK)	PRKAA1	8bik	-4.7
	Absent in Melanoma 2	AIM2	3vd8	-4.3
	Piezo-type mechanosensitive ion channel component 1	PIEZO1	Q92508	-4.4

2.10. Histopathological analysis

Isolated lung tissue samples will be serially sectioned with a microtome at 3 μ m thickness, fixed in 10% neutral buffered formalin (pH 7.4) for 72 hours, washed, dehydrated, embedded in paraffin wax, and stained with hematoxylin and eosin (H&E) for histopathological evaluation.

2.11. Immunohistochemical detection of NF- κ B expression

The lung paraffin slices, measuring 5 μ m in thickness, were deposited onto glass slides with a positive charge using the avidin-biotin-peroxidase complex (ABC) technique. These sections were subsequently used for the purpose of identifying primary antibodies NF- κ B (1:100). The sections underwent paraffin removal treatment, followed by hydration using progressively lower amounts of alcohol. Afterwards, they were subjected to a 3% hydrogen peroxide solution for a duration of 10 minutes in order to deactivate the natural peroxidase. The process of antigen retrieval involved immersing the sections in a Tris buffered saline solution (0.05 M, pH 7.6) for a duration of 5 minutes, followed by cooling at room temperature for a period of 10 minutes. Ultimately, the pieces undergo a 1-minute rinsing process using PBS.

After the sections were washed, a secondary antibody, specifically a biotinylated goat antipolyvalent antibody, was applied for a period of 10 minutes. To detect the antigen-antibody complex, the marker expression was tagged with peroxidase and subsequently stained with DAB chromogen. Then, the sections were treated with Mayer's hematoxylin in order to apply a counterstain. By using Olympus microscope (BX-53), cells that displayed positive signals were the only ones that exhibited a noticeable brown immunostaining. The immunohistochemistry data were evaluated by calculating the percentage of reaction area in 10 microscopic fields using *image J* software (Version 1.4.3.67).

2.12. Statistical analysis

The statistical software tool (SPSS) version 23.0, created by SPSS, Inc. in Chicago, IL, USA, was used to analyze the data. The One-way analysis of variance (ANOVA) was employed to examine the differences among parametric data. To address the issue of numerous comparisons, a post-hoc test known as Tukey's Honestly Significant Difference (HSD) was utilized. The mean \pm standard deviation (S.D.) was used to report the values, with a statistical significance of $p < 0.05$.

3. Results

3.1. The network pharmacology analysis

3.1.1. Defining the targets related to 5-aminolevulinic acid

We examined four databases to find the targets connected to 5-ALA. A total of 319 targets were identified; these targets came from 100 (SwissTargetPrediction), 91 from SuperPred, 3 from DrugBank, and 125 from TargetNet. After duplicates were removed, there were 282 targets remaining (**Supplementary Table S3, Fig.1.A**).

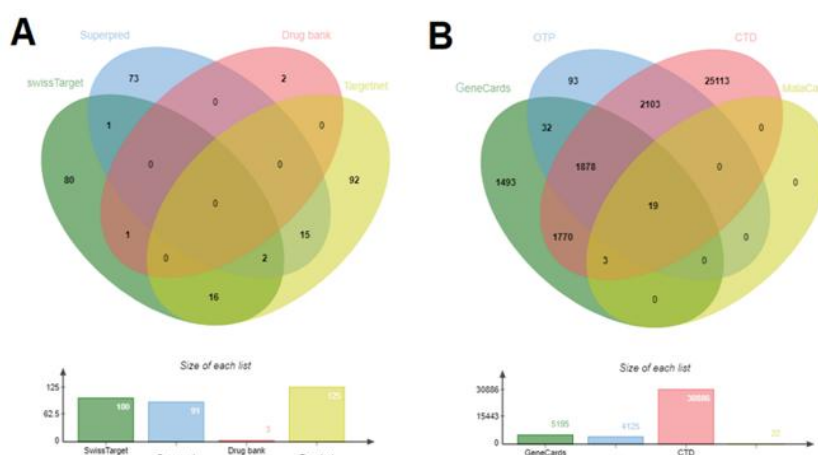


Fig.1. Targets associated with 5-aminolevulinic acid and chronic obstructive pulmonary disease

(A) The targets connected to “5-aminolevulinic acid (5-ALA)”; collected from the four databases SwissTargetPrediction, SuperPred, DrugBank, and TargetNet; and (B) the targets linked to “chronic obstructive pulmonary disease (COPD)”; gathered from the four databases GeneCards, OpenTargets Platform, Comparative Toxicogenomics Database (CTD), and MalaCards

3.1.3. Targets of 5-ALA overlapped with COPD

Among the 282 targets for 5-ALA and 32504 targets for COPD, 273 unique targets were noticed (**Supplementary Table S6, Fig.2.A**).

3.1.4. Protein–Protein Interaction (PPI) Network of the 273 Drug-Diseases overlapped Targets

By uploading all 273 overlapping targets to the STRING database, a PPI diagram was created to show how they interact with one another, where it consisted of 273 nodes and 1948 edges (**Fig.2.B**). After the targets were sorted by String protein node degree and filtered using the Degree-median filtration (Degree>11), the 138 targets were detected. Then, the network was

3.1.2. Determining the targets associated with COPD

Furthermore, a thorough examination of four databases was carried out to identify the targets connected to COPD. The GeneCards database provided 5195 targets, the OpenTargets Platform database provided 4125, the Comparative Toxicogenomics Database: CTD provided 30886, and the MalaCards database produced 22 of the total 40228 targets. Following the elimination of duplicate entries, there were only 32504 targets in total (**Supplementary Table S5, Fig.1.B**).

integrated using Cytoscape program 3.10.2 to conduct further investigation. Using the CytoNCA software, the 138 targets were ranked based on Degree value, Betweenness and Closeness (**Supplementary Table S6**). After that, a drug-targets network of the 138 common targets was built using Cytoscape (**Fig.2.C**). Likewise, a PPI network incorporating the top 10 hub targets (CASP3, HIF1A, PTGS2, NFKB1, TLR4, SIRT1, MTOR, GRIN2B, RELA, and PRKACA) and the experimentally verified targets (AMPK (PRKAA1), Nrf2 (NFE2L2), AIM2, IL1 α (IL1A), Piezo1, NFKB (NFKB1), TNF- α (TNF), and IL-6) was established (**Fig.2.D**).

3.1.5. Enrichment analysis of the related proteins

The ShinyGO program was utilized to conduct GO enrichment analysis to verify the significant biological and functional characteristics of the relevant 138 proteins.

For biological processes (BP), cellular components (CC), and molecular functions (MF), statistical enrichment analysis with a P value < 0.05 was performed (**Supplementary Table S7, Fig.2.E-G**). Top BP included regulation of biological quality, response to oxygen-containing compound, and cellular response to chemical stimulus; Top CC was postsynaptic membrane, synaptic membrane, synapse, and somatodendritic compartment; Top MF included glutamate receptor activity, G protein-coupled glutamate receptor activity, adenylate cyclase inhibiting G protein-coupled glutamate receptor activity, and molecular transducer activity.

To determine the likely pathways associated with the effect of 5-ALA against COPD, a KEGG pathway analysis was performed with a P value < 0.05. This analysis included the top 10 hub targets with the eight experimentally verified targets. Among the top 30 KEGG Pathways implicated in the pathophysiology of COPD were the NF-kappaB binding and the TNF signaling pathways (**Supplementary Table S7, Fig.2.H**). Notably, it was also discovered that these pathways were connected to a few of the targets that had been experimentally verified, including IL1A, NFKB, TNF, and IL-6 (**Fig.2.I&J**).

3.1.6. Molecular docking confirmed the relationship between 5-ALA and experimentally validated targets

To verify that the 5-ALA molecule is associated with the other indicated targets

(PRKAA1, AIM2, and Piezo1), the docking approach investigation was carried out. The results showed that the most active and binding-affinity-strong models of PRKAA1, AIM2, and Piezo1 had reduced binding energies of -4.7, -4.3, and -4.4 kcal/mol, respectively (**Supplementary Table S8, Table 2; Fig.3**).

3.2. 5-ALA enhanced lung AMPK expression in a rat model of LPS-induced COPD

The findings of the study revealed that rats injected with LPS exhibited a statistically significant reduction in AMPK expression in comparison to control group. Conversely, the administration of 5-ALA resulted in a notable augmentation in the expression of AMPK in LPS+5-ALA group ($p < 0.05$; **Fig. 4A**).

3.3. 5-ALA upregulated lung Nrf2 expression in a rat model of LPS-induced COPD

The data of the study revealed that the administration of LPS to rats caused a substantial drop in lung Nrf2 gene expression when compared to control group. In contrast, providing 5-ALA resulted in a notable elevation Nrf2 expression compared to LPS group ($p < 0.05$; **Fig.5A**).

3.4. 5-ALA mitigated the alterations in lung oxidant/antioxidant status in a rat model of LPS-induced COPD

In comparison to control group, rats that received LPS demonstrated a considerable elevation in MDA level, accompanied by a marked decrease in HO-1 concentration and TAC. The concentration of MDA was found to be significantly decreased in LPS+5-ALA group compared to LPS group, with an increase in HO-1 level and TAC ($p < 0.05$; **Fig. 5B, C&D**).

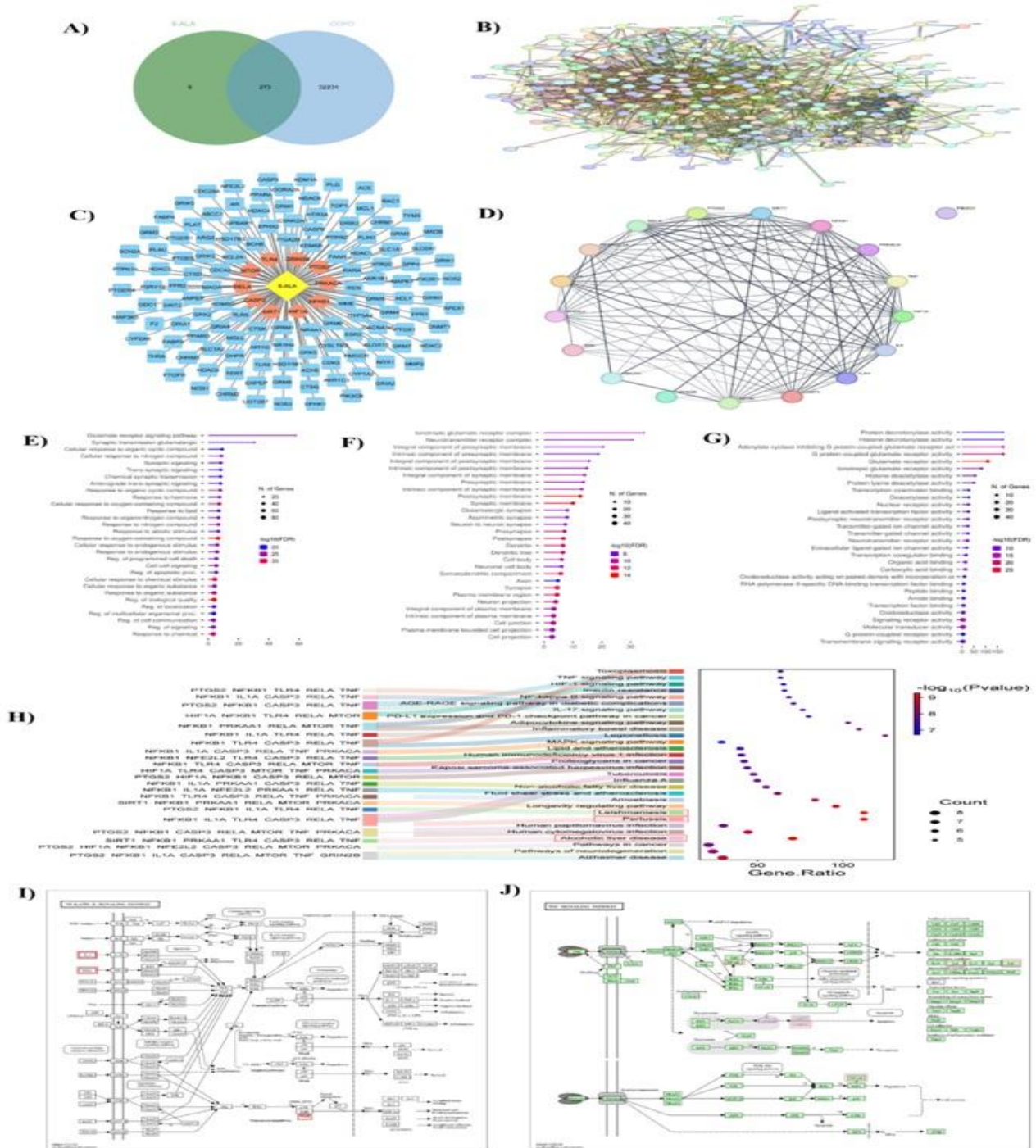


Fig.2. Network pharmacology analysis

(A) The 273 intersection targets overlap with “5-aminolevulinic acid (5-ALA)” and “chronic obstructive pulmonary disease (COPD)”, (B) A protein-protein interaction (PPI) network consisting of 273 linked targets was constructed using 273 nodes and 1948 edges. The average node degree was 14.3, after excluding the unconnected nodes. The interaction score was established at 0.4, representing medium confidence and serving as the default level. (C) The drug-targets network, **Diamond**: drug, **Oval**:10 hub targets (CASP3, HIF1A, PTGS2, NFKB1, TLR4, SIRT1, MTOR, GRIN2B, RELA, and PRKACA), **Ellipse**: other overlapped targets, (D) The PPI network of 10 hub targets and experimentally validated targets (AMPK (PRKAA1), Nrf2 (NFE2L2), AIM2, IL1 α (IL1A), Piezo1, NFKB (NFKB1), TNF- α (TNF), and IL-6), (E), (F), &(G)the top 30 significantly enriched Gene Ontology (GO) analyses (sorted by P value) including biological process (BP), cellular component (CC), and molecular function (MF), respectively, (H) KEGG pathways (sorted by P value), (I) NF-kappaB binding pathway, and (J) TNF signaling pathway.

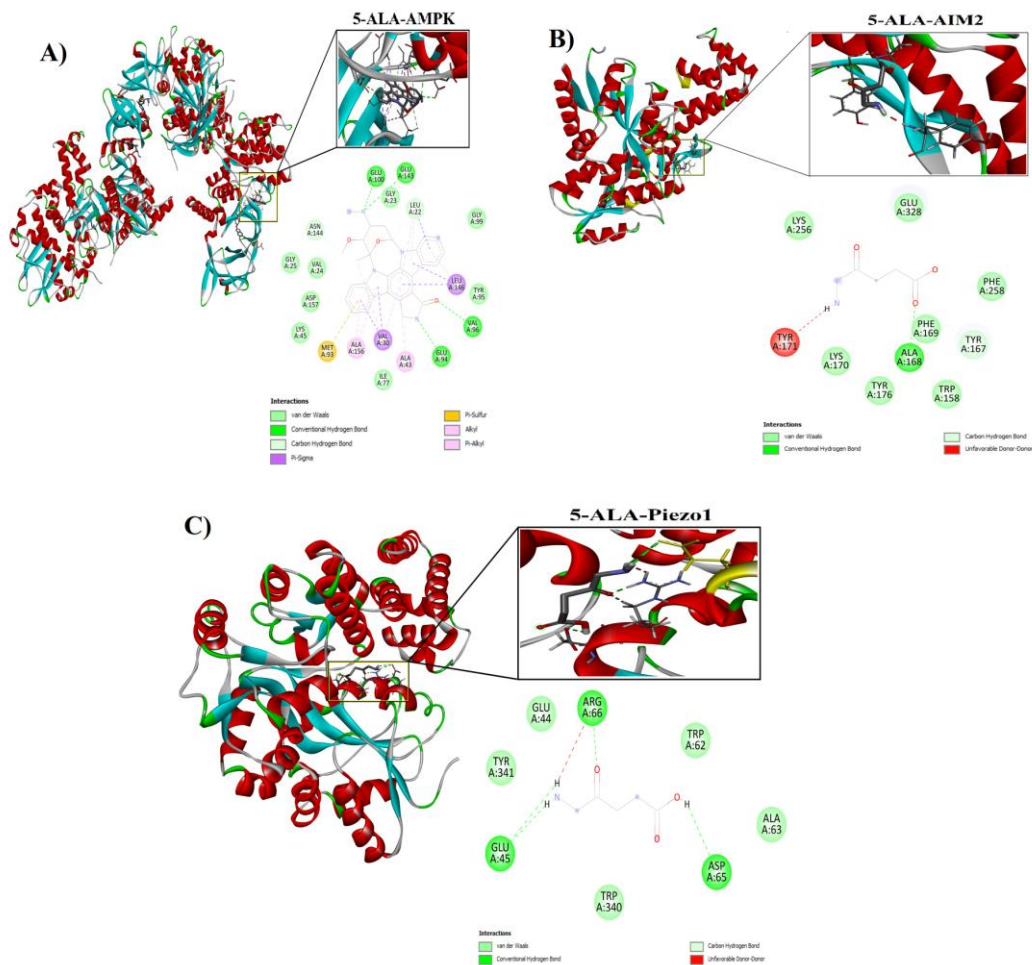


Fig.3. The predicted three- and two-dimensional binding models of 5-aminolevulinic acid (5-ALA) binding to protein targets. Molecular docking results of 5-ALA with (A) PRKAA1/AMPK (**PBD ID:** 8bik), (B) AIM2 (**PBD ID:** 3vd8), and (C) PIEZO1 (**PBD ID:** Q92508). **PRKAA1/AMPK**; AMP-activated protein kinase, **AIM2**; Absent in Melanoma 2, and **PIEZO1**; Piezo-type mechanosensitive ion channel component 1

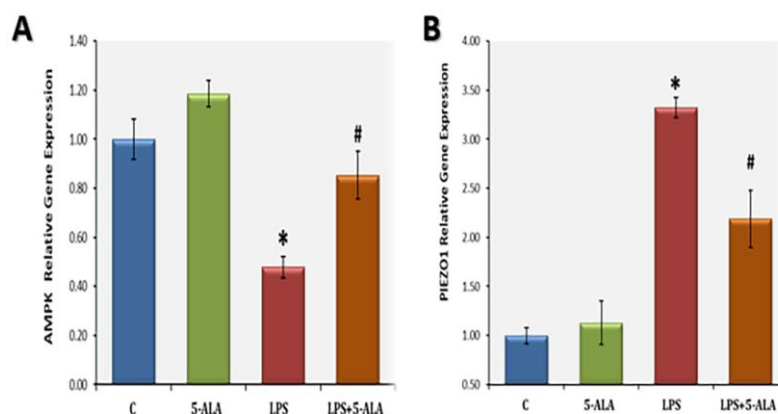


Fig.4.Effect of 5-ALA on relative gene expression of AMPK, and Piezo1in lung tissue in a rat model of LPS-induced COPD (A) AMPK expression& (B) Piezo1 expression. Values were expressed as means ± SD. Significant difference vs.*C or #LPS groups, each at $p < 0.05$; using One-way ANOVA followed by Tukey's Honestly Significant Difference (HSD)post hoc. **AMPK**; AMP-activated kinase, **Nrf2**; Nuclear factor erythroid 2-related factor 2.C; Control, **5-ALA**;5-aminolevulinic acid, and **LPS**; Lipopolysaccharide

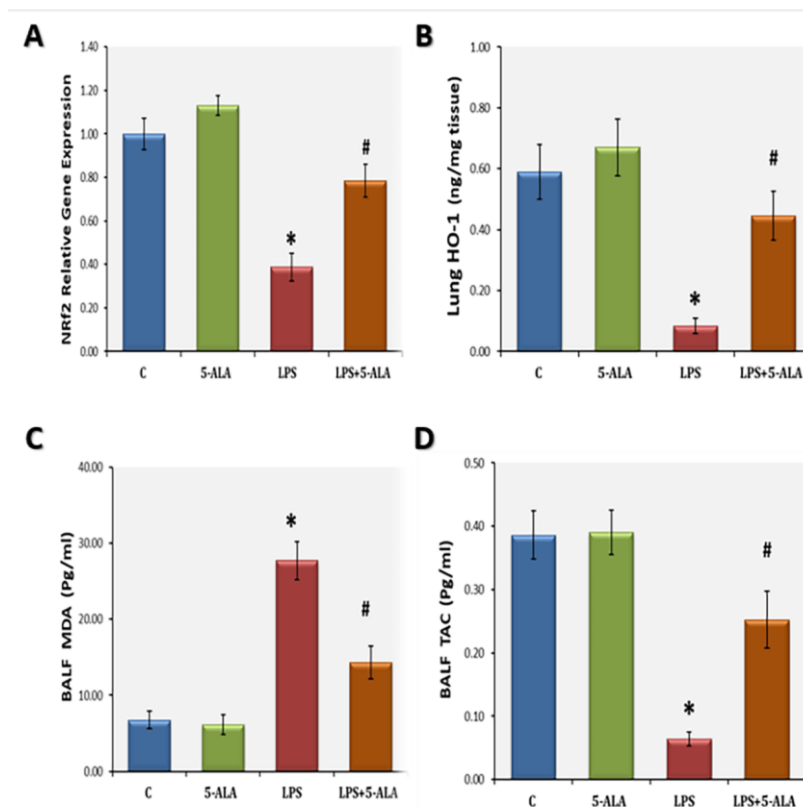


Fig.5.Effect of 5-ALA on BALF and lung oxidant/antioxidant status in a rat model of LPS-induced COPD

(A) Bar graph reflecting Nrf2 expression, (B) HO-1 level (ng/mg tissue), (C) MDA level (nmol/ml), and (D) TAC (μ mol/ml). Values were expressed as means \pm SD. Significant difference vs. [#]C or ^{*}LPS groups, each at $p < 0.05$; using One-way ANOVA followed by Tukey's Honestly Significant Difference (HSD) post-hoc. Nrf2; Nuclear factor erythroid 2-related factor 2, HO-1; Heme oxygenase-1, MDA; Malondialdehyde, and TAC; Total antioxidant capacity. C; Control, 5-ALA; 5-aminolevulinic acid, and LPS; Lipopolysaccharide

3.5. 5-ALA minimized lung AIM2/IL1 α /Piezo1 signaling pathway in a rat model of LPS-induced COPD

The observations we collected showed that the COPD group exhibited a significant increase in IL1 α level. Also, there was upregulation in the expression of AIM2 and Piezo1 in comparison to control group. By contrast, feeding rats with 5-ALA resulted in a notable decline in IL1 α level, as well as AIM2 and Piezo1 expression relative to LPS group ($p < 0.05$; Fig.7, Fig.6.A& Fig.4.B).

3.6.5-ALA suppressed the lung inflammatory cytokines in a rat model of LPS-induced COPD

Referring to our results, it was observed that following LPS exposure, TNF- α and IL-6 levels were considerably higher than in control

group. Unlike LPS group, the administration of 5-ALA resulted in a significant decrease in TNF- α and IL-6 levels (Fig.6.B&C).

The findings indicated that control group displayed negative immunopositive reactions to NF- κ B in its lung tissue. However, LPS-injected rats showed obvious immunopositive reactions to NF- κ B. In contrast to control group, rats of LPS+5-ALA group showed moderate reactions to NF- κ B. Similar to the findings shown in the photographic sections, the quantitative analysis demonstrated notable increases in NF- κ B expression in rats exposed to LPS, as compared to control group. Conversely, the expression of NF- κ B was markedly reduced in rats that were administered 5-

ALA, in comparison to COPD group ($p < 0.05$; Fig.9).

3.7.5-ALA ameliorated the histological changes observed in the lung tissues within a rat model of LPS-induced COPD

The lung in the control and 5-ALA groups showed a normal lung histological architecture. Contrarily, lung tissues from rats exposed to LPS displayed bronchostenosis due to marked

lymphoid peribronchial hyperplasia and marked obliteration of lumen of bronchioles by debris. Narrowed alveoli and thickened alveolar septa were seen. Rats in LPS+5-ALA group, on the other hand, presented normal alveolar lumen, alveolar septa, alveolar sacs but bronchioles with very minimal peribronchial infiltration and minimal obliteration of the lumen by debris still seen (Fig. 8).

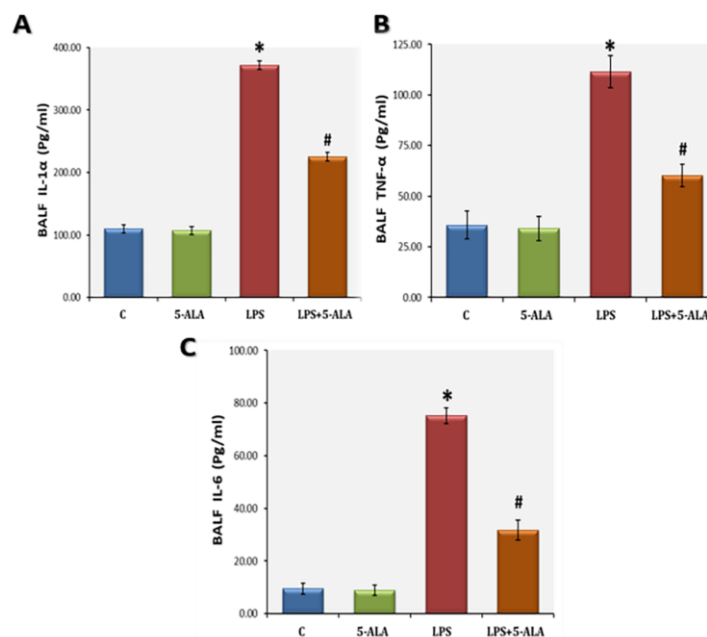


Fig.6.Effect of 5-ALA on BALF levels of inflammatory cytokines in a rat model of LPS-induced COPD (A) IL-1α level (pg/ml), (B) TNF-α level (pg/ml), (C) IL-6 level (pg/ml). Values were expressed as means ± SD. Significant difference vs. *C or #LPS groups, each at $p < 0.05$; using One-way ANOVA followed by Tukey's Honestly Significant Difference (HSD) post-hoc. TNF-α; Tumor necrosis factor alpha, IL-1α; Interleukin-1-alpha and IL-6; Interleukin-6. C; Control, 5-ALA; 5-aminolevulinic acid, and LPS; Lipopolysaccharide

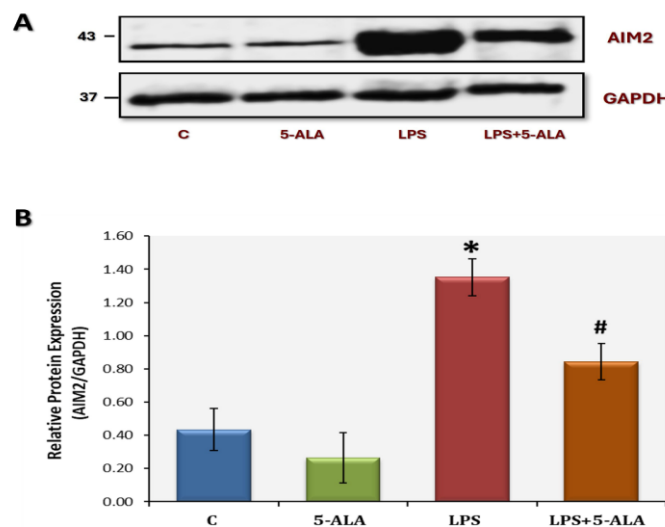


Fig.7.Effect of 5-ALA on lung AIM2 expression in a rat model of LPS-induced COPD

(A) Western blot & (B) Bar graph reflecting AIM2 expression. Values were expressed as means \pm SD. Significant difference vs. [#]C or ^{*}LPS groups, each at $p < 0.05$; using One-way ANOVA followed by Games-Howell post-hoc. AIM2, Absent in melanoma 2 inflammasome. C; Control, 5-ALA; 5-aminolevulinic acid, and LPS; Lipopolysaccharide

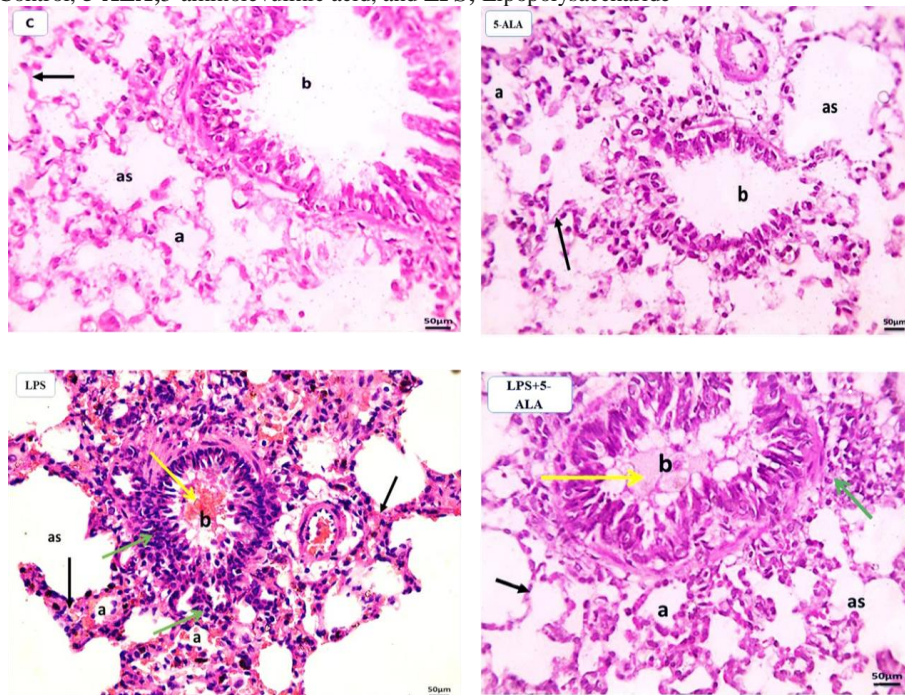


Fig.8. Photomicrographs demonstrating the effect of 5-ALA on the histopathological alterations in lung tissue sections of a rat model of LPS-induced COPD (Hematoxylin and Eosin Stain, Magnification Power= x 400, Scale bar=50 μ m); Lung tissue; Rat. Lung Sections from C, 5-ALA, LPS, and LPS+5-ALA groups highlighted the changes between groups. LPS showing bronchostenosis due to marked lymphoid peribronchial hyperplasia (green arrow), lumen obliteration by cellular debris (yellow arrow), collapsed alveoli (a), thickened alveolar septa (black arrow) and enlarged alveolar sacs (as). C, 5-ALA and LPS+5-ALA groups showed normal alveoli (a), alveolar septa (black arrows) and bronchioles (b) mild peribronchial infiltration (green arrow) and some debris in the lumen (yellow arrow) are seen. C; Control, 5-ALA; 5-aminolevulinic acid, and LPS; Lipopolysaccharide

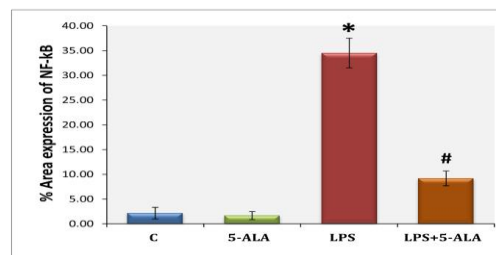
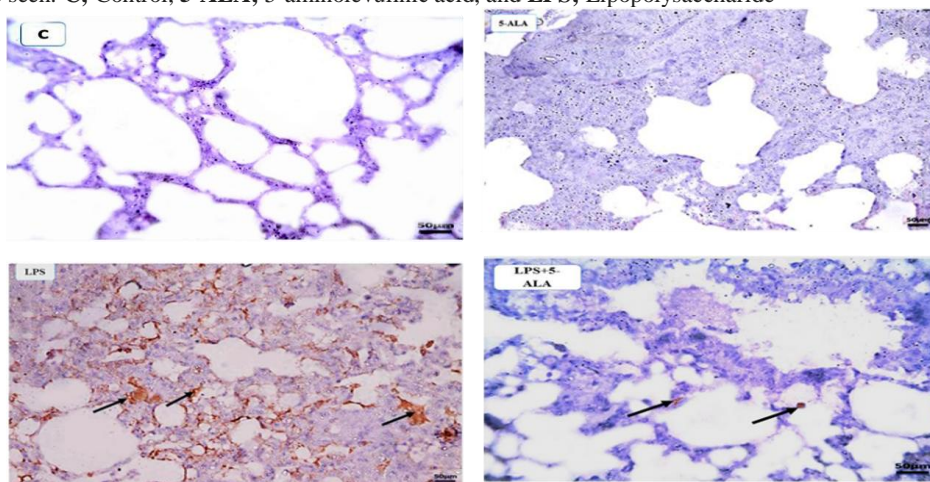


Fig.9. Photomicrographs showing the effect of 5-ALA on NF- κ B immunostaining in lung tissue sections of a rat model of LPS-induced COPD; (Magnification Power= x 400, Scale bar=50 μ m); Lung tissue; Rat. Lung Sections revealed the presence of negative cytoplasmic and nuclear expressions of NF- κ B in C&5-ALA groups but marked positive reaction (arrows) in LPS group, and moderate reaction (arrows) in LPS+5-ALAgrou. Chart representing the quantitative

scoring of NF- κ B. Values were expressed as means \pm SD. Significant difference vs. *C or #LPS groups, each at $p < 0.05$; using One-way ANOVA followed by Tukey's Honestly Significant Difference (HSD) post-hoc. C; Control, 5-ALA; 5-aminolevulinic acid, and LPS; Lipopolysaccharide

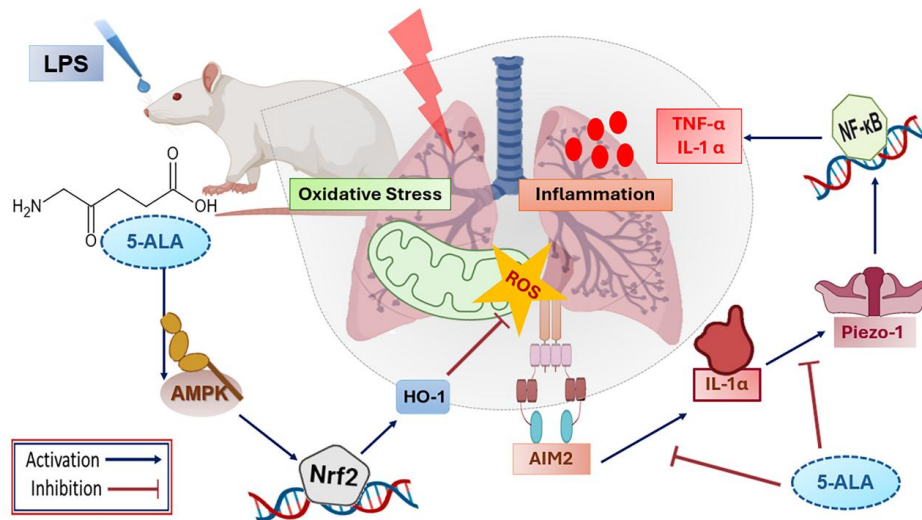


Fig.10. A schematic diagram showing the mitigating effect of 5-ALA against LPS-induced COPD.

5-aminolevulinic acid(5-ALA) may ameliorates lipopolysaccharide (LPS)-induced inflammatory insult, through upregulating AMPK expression and therefore, activating Nrf2/ Ho-1 axis with diminished oxidative stress. Consequently, minimized ROS overproduction could block AIM2/IL1 α /Piezo1 signaling, which in turn prohibit NF- κ B expression and associated outflow of inflammatory cytokines (TNF α and IL-6).

4. Discussion

Various animal systems have been established for studying COPD, including a model that uses tobacco smoke, a model involves inhaling pollutants, and a lipopolysaccharide (LPS) model. However, establishing an LPS model is comparatively simpler and less time consuming than establishing other models[3]. Prior studies have demonstrated the importance of 5-Aminolevulinic acid (5-ALA) against inflammatory diseases. 5-ALA supplementation could suppress inflammatory reactions and alleviate associated organ injury[17,18]. Especially there is no report clarified the potential helpful effect of 5-ALA against LPS-induced COPD in rats. A suppressing influence of 5-ALA on AIM2/IL1 α /Piezo1 signaling axis, via AMP-activated kinase (AMPK) activation, has been clarified as novel mechanism for its potential pulmonary therapeutic role (**Fig.10**).

In this work, the key targets and pathways implicated in the impact of 5-ALA against COPD were predicted and investigated using a network pharmacology and molecular docking modeling approach. The outcomes showed some degree of agreement between the conclusions of the network analysis and the results of the in-vivo experiment. The study indicated that CASP3, HIF1A, PTGS2, NFKB1, TLR4, SIRT1, MTOR, GRIN2B, RELA, and PRKACA were the top 10 hub targets linked to 5-ALA and COPD. Plus, network analysis demonstrated a high association between the onset of COPD and a number of signaling pathways, including NF-kappaB binding and TNF signaling pathways.

The PPI research revealed an intense association between some of the experimentally verified targets and other targets related to potential pathways influencing the development of COPD. These targets included Nrf2 (NFE2L2), IL1 α (IL1A), NFKB (NFKB1), TNF- α (TNF), and

IL-6. Simultaneously, the affinity of 5-ALA for AMPK (PRKAA1), AIM2, and Piezo1 has been examined and assessed using molecular docking. Docking studies have verified that 5-ALA has a high inclination to bind to these targets. Using the first data obtained from network analysis and docking studies, we have formulated a strategy to conduct in-vivo investigation to support our preliminary hypothesis.

Results of the current study affirm that administrating 5-ALA to LPS rats for two weeks, dramatically increased AMPK levels, which recently exhibit a significant protective effect in preventing lung injury and minimize endoplasmic reticulum (ER) stress under inflammatory instances[33, 34]. 5-ALA has been recorded as an activator of AMPK signaling [17]. Activated AMPK has been demonstrated to positively regulate Nrf2/HO-1 signaling pathway[35]. Since activation of AMPK triggers its-dependent effectors, as PGC-1 α , which has a regulatory role in enhancing the expression of Nrf2 by inhibiting GSK3 β [36, 37]. Nrf2 is a key transcription factor that plays a crucial role in combating oxidative stress by activating the production of downstream anti-oxidative genes, such as HO-1[38]. The link between AMPK and Nrf2 is crucial for preserving cellular redox balance against oxidative stress.

It is known that LPS induces the generation of reactive oxygen species (ROS), provoking oxidative stress, which is a significant contributing mechanism of COPD. Oxidative stress arises from a disparity between ROS generation and the body's capacity to counteract them with antioxidant mechanisms, resulting in cellular damage [39, 40]. Conversely, receiving 5-ALA led to a notable reduction in lung MDA,

accompanied by a considerable increase in TAC and HO-1 levels. This considerably impeded the advancement of oxidative stress, in agreement with [21].

Excessive ROS production can act as a signal to activate the AIM2 inflammasome[14], which in turn stimulates IL-1 α secretion[10]. It's worth noting that the expression and function of Piezo1 gene are enhanced by inflammatory signaling initiated by IL-1 α . When Piezo1 is activated, it leads to influx of cations (as calcium) into the cell, thereby starting downstream signaling cascades. These pathways can influence the expression of genes, including that of NF- κ B[7, 9].

Current research is focused on investigating the interaction between Piezo1 and NF- κ B. There is growing evidence indicating that mechanical signaling mediated by Piezo1 might affect NF- κ B activity, influencing inflammation and immunological responses[6, 7]. NF- κ B activation leads to an elevation in the production of inflammatory cytokines such as TNF- α and IL-6[41]. However, our results showed reduced Piezo1 and NF- κ B expression with decreased brain levels of AIM2, IL-1 α , TNF- α , and IL-6 in 5-ALA groups. Based on previously mentioned mechanisms, these anti-inflammatory actions can be explained by increasing AMPK levels, by 5-ALA administration, which leads to upregulation of Nrf2, followed by suppression of AIM2/IL1 α /Piezo1 signaling pathway.

Therefore, AMPK activation with subsequent inhibition of AIM2/IL1 α /Piezo1 axis could attenuate LPS-induced oxidative stress and inflammatory reactions. Considering these data provided, it is reasonable to anticipate that rats treated with 5-ALA in the current study will

exhibit less histopathological alterations in their lung tissues compared to the LPS-COPD rats. They showed improvement of the histological structure of the lung tissue as reduction of inflammatory cellular infiltration which may be potentially related to its anti-inflammatory property.

5. Conclusion

Collectively, network pharmacology, molecular docking, and in-vivo experimental validation provide evidence on the involvement of AIM2/IL1 α /Piezo1 signaling pathway in the pathogenesis of LPS-induced COPD in rats. Further, it shed light on the potential effective role of 5-ALA through AMPK-mediated mechanisms. By stimulating AMPK, 5-ALA could increase the activity Nrf2/HO-1, and ultimately block AIM2/IL1 α /Piezo1 axis. This suppresses the activation of genes regulated by Piezo1, like NF- κ B, therefore reducing its related inflammatory cascade.

CRedit authorship contribution statement

Maram M. El Tabaa: Conception, study design, methodology, data analysis and/or interpretation, drafting and revising the manuscript. **Manar M. El Tabaa:** Network pharmacology and molecular docking methodology, results data analysis and/or interpretation. **Ahmed Almeldin, Yasmeen M. El-Harty:** Study design, methodology, drafting and revising the manuscript. **Hoda M. Ibrahim:** Methodology-real-time RT-PCR technique and data analysis. **Maram M. Ghabrial:** Methodology-histopathological and immunohistochemical examination and revising the manuscript.

Consent for publication

All the authors reviewed and agreed to the publication of the manuscript.

Declaration of Competing Interest

The authors declare that they have no competing financial interests or personal relationships that could have appeared to influence the work reported in this manuscript.

Funding

Not applicable

Data availability

Data will be made available on request.

References

1. **Song H, Jiang L, Yang W, et al** Cryptotanshinone alleviates lipopolysaccharide and cigarette smoke-induced chronic obstructive pulmonary disease in mice via the Keap1/Nrf2 axis. *Biomed Pharmacother* 165:115105, 2023
2. **Zeng D, Zhang W, Chen X, et al** Inhibitory Effect of P22077 on Airway Inflammation in Rats with COPD and Its Mechanism. *Int J COPD* 19:779–788, 2024
3. **Lee SY, Cho JH, Cho SS, et al** Establishment of a chronic obstructive pulmonary disease mouse model based on the elapsed time after LPS intranasal instillation. *Lab Anim Res* 34:1, 2018
4. **Li L, Yang L, Yang L, et al** Network pharmacology: a bright guiding light on the way to explore the personalized precise medication of traditional Chinese medicine. *Chinese Med* 2023 18:1–19, 2023
5. **Xiong H, Yang J, Guo J, et al** Mechanosensitive Piezo channels mediate the physiological and pathophysiological changes in the respiratory system. *Respir Res* 23:1–9, 2022

6. **Tang Y, Zhao C, Zhuang Y, et al** Mechanosensitive Piezo1 protein as a novel regulator in macrophages and macrophage-mediated inflammatory diseases. *Front Immunol* 14:1149336, 2023
7. **Sun Y, Leng P, Song M, et al** Piezo1 activates the NLRP3 inflammasome in nucleus pulposus cell-mediated by Ca²⁺/NF- κ B pathway. *Int Immunopharmacol* 85:106681, 2020
8. **Schuliga M** NF-kappaB Signaling in Chronic Inflammatory Airway Disease. *Biomolecules* 5:1266, 2015
9. **Lee W, Nims RJ, Savadipour A, et al** Inflammatory signaling sensitizes Piezo1 mechanotransduction in articular chondrocytes as a pathogenic feed-forward mechanism in osteoarthritis. *Proc. Natl. Acad. Sci. U. S. A.* 118:, 2021
10. **Colarusso C, Terlizzi M, Molino A, et al** AIM2 inflammasome activation leads to IL-1 α and TGF- β release from exacerbated chronic obstructive pulmonary disease-derived peripheral blood mononuclear cells. *Front. Pharmacol.* 10:, 2019
11. **Osei ET, Brandsma CA, Timens W, Heijink IH, Hackett TL** Current perspectives on the role of interleukin-1 signalling in the pathogenesis of asthma and COPD. *Eur. Respir. J.* 55:, 2020
12. **Wang J, Li R, Peng Z, et al** HMGB1 participates in LPS-induced acute lung injury by activating the AIM2 inflammasome in macrophages and inducing polarization of M1 macrophages via TLR2, TLR4, and RAGE/NF- κ B signaling pathways. *Int J Mol Med* 45:61–80, 2020
13. **Taniguchi A, Tsuge M, Miyahara N, Tsukahara H** Reactive Oxygen Species and Antioxidative Defense in Chronic Obstructive Pulmonary Disease. *Antioxidants* 10:, 2021
14. **Crane DD, Bauler TJ, Wehrly TD, Bosio CM** Mitochondrial ROS potentiates indirect activation of the AIM2 inflammasome. *Front Microbiol* 5:107836, 2014
15. **Zimmermann K, Baldinger J, Mayerhofer B, et al** Activated AMPK boosts the Nrf2/HO-1 signaling axis—A role for the unfolded protein response. *Free Radic Biol Med* 88:417, 2015
16. **Mo C, Wang L, Zhang J, et al** The Crosstalk Between Nrf2 and AMPK Signal Pathways Is Important for the Anti-Inflammatory Effect of Berberine in LPS-Stimulated Macrophages and Endotoxin-Shocked Mice. <https://home.liebertpub.com/ars> 20:574–588, 2014
17. **Yu H, Zhang M, Ma Y, et al** 5-ALA ameliorates hepatic steatosis through AMPK signaling pathway. *J Mol Endocrinol* 59:121–128, 2017
18. **Fujino M, Nishio Y, Ito H, Tanaka T, Li XK** 5-Aminolevulinic acid regulates the inflammatory response and alloimmune reaction. *Int Immunopharmacol* 37:71–78, 2016
19. **Otaka Y, Kanai K, Okada D, et al** Effects of Oral 5-Aminolevulinic Acid on Lipopolysaccharide-Induced Ocular Inflammation in Rats. *Vet Sci* 2023, Vol

- 10, Page 207 10:207, 2023
20. **Chen J, Wang H, Wu Z, et al** Effects of 5-aminolevulinic acid on the inflammatory responses and antioxidative capacity in broiler chickens challenged with lipopolysaccharide. *animal* 16:100575, 2022
 21. **Matsuo K, Yabuki Y, Fukunaga K** 5-aminolevulinic acid inhibits oxidative stress and ameliorates autistic-like behaviors in prenatal valproic acid-exposed rats. *Neuropharmacology* 168:107975, 2020
 22. **Al-Harbi NO, Imam F, Al-Harbi MM, et al** Protective effect of Apremilast against LPS-induced acute lung injury via modulation of oxidative stress and inflammation. *Saudi J Biol Sci* 29:3414–3424, 2022
 23. **Kesecioglu J, Schultz MJ, Haitsma JJ, den Heeten GJ, Lachmann B** Lodixanol inhibits exogenous surfactant therapy in rats with acute respiratory distress syndrome. *Eur Respir J* 19:820–826, 2002
 24. **Rappaport N, Fishilevich S, Nudel R, et al** Rational confederation of genes and diseases: NGS interpretation via GeneCards, MalaCards and VarElect. *Biomed. Eng. Online* 16:, 2017
 25. **Szklarczyk D, Kirsch R, Koutrouli M, et al** The STRING database in 2023: protein-protein association networks and functional enrichment analyses for any sequenced genome of interest. *Nucleic Acids Res* 51:D638–D646, 2023
 26. **Shannon P, Markiel A, Ozier O, et al** Cytoscape: A Software Environment for Integrated Models of Biomolecular Interaction Networks. *Genome Res* 13:2498, 2003
 27. **Tang Y, Li M, Wang J, Pan Y, Wu FX** CytoNCA: a cytoscape plugin for centrality analysis and evaluation of protein interaction networks. *Biosystems* 127:67–72, 2015
 28. **Ge SX, Jung D, Jung D, Yao R** **ShinyGO**: a graphical gene-set enrichment tool for animals and plants. *Bioinformatics* 36:2628–2629, 2020
 29. **Tang D, Chen M, Huang X, et al** **SRplot**: A free online platform for data visualization and graphing. *PLoS One* 18:, 2023
 30. **Torres PHM, Sodero ACR, Jofily P, Silva-Jr FP** Key Topics in Molecular Docking for Drug Design. *Int J Mol Sci* 2019, Vol 20, Page 4574 20:4574, 2019
 31. **Ohkawa H, Ohishi N, Yagi K** Assay for lipid peroxides in animal tissues by thiobarbituric acid reaction. *Anal Biochem* 95:351–358, 1979
 32. **Koracevic D, Koracevic G, Djordjevic V, Andrejevic S, Cosic V** Method for the measurement of antioxidant activity in human fluids. *J Clin Pathol* 54:356–361, 2001
 33. **Becker E, Husain M, Bone N, et al** AMPK activation improves recovery from pneumonia-induced lung injury via reduction of er-stress and apoptosis in alveolar epithelial cells. *Respir Res* 24:1–15, 2023
 34. **Zhang Z, Deng X, Gu W, et al** Jianghu decoction and its active component polydatin inhibit inflammation and fibrotic

- lesions in the lungs of ILD mice via the AMPK signaling pathway. *J Ethnopharmacol* 318:117003, 2024
35. **Zimmermann K, Baldinger J, Mayerhofer B, et al** Activated AMPK boosts the Nrf2/HO-1 signaling axis—A role for the unfolded protein response. *Free Radic Biol Med* 88:417, 2015
36. **Gureev AP, Shaforostova EA, Popov VN** Regulation of Mitochondrial Biogenesis as a Way for Active Longevity: Interaction Between the Nrf2 and PGC-1 α Signaling Pathways. *Front. Genet.* 10:, 2019
37. **Rabinovitch RC, Samborska B, Faubert B, et al** AMPK Maintains Cellular Metabolic Homeostasis through Regulation of Mitochondrial Reactive Oxygen Species. *Cell Rep* 21:1–9, 2017
38. **Zhang Y, Wang J, Wang Y, Lei K** Nrf2/HO-1 signaling activation alleviates cigarette smoke-induced inflammation in chronic obstructive pulmonary disease by suppressing NLRP3-mediated pyroptosis. *J Cardiothorac Surg* 19:1–9, 2024
39. **Barnes PJ** Oxidative Stress in Chronic Obstructive Pulmonary Disease. *Antioxidants* 11:, 2022
40. **Wang Y, Chen J, Chen W, et al** LINC00987 Ameliorates COPD by Regulating LPS-Induced Cell Apoptosis, Oxidative Stress, Inflammation and Autophagy Through Let-7b-5p/SIRT1 Axis. *Int J Chron Obstruct Pulmon Dis* 15:3213, 2020
41. **Liu T, Zhang L, Joo D, Sun SC** NF- κ B signaling in inflammation. *Signal Transduct. Target. Ther.* 2:, 2017